CrossMark

Preparation of thiourea-intercalated kaolinite and its influence on thermostability and flammability of polypropylene composite

Wufei Tang[1], Lixiang Song[1,2], Sheng Zhang[1,2], Hongfei Li[1], Jun Sun[1], and Xiaoyu Gu[1,*]

[1] Key Laboratory of Carbon Fiber and Functional Polymers, Ministry of Education, Beijing University of Chemical Technology, Beijing 100029, People's Republic of China
[2] Centre for Fire Safety Materials, Beijing University of Chemical Technology, Beijing 100029, People's Republic of China

ABSTRACT

A novel thiourea-intercalated kaolinite flame retardant (K-TU) was prepared by intercalating thiourea (TU) into kaolinite. The structure of K-TU was characterized by Fourier transform infrared spectroscopy, thermogravimetric analysis (TGA), and X-ray diffraction. K-TU in association with intumescent flame retardants (IFR) was then introduced into polypropylene (PP) by melt blending. The flammability and thermostability were evaluated by limiting oxygen index (LOI), vertical burning test (UL-94), cone calorimetry (Cone), and TGA. The results showed that the sample PP/23.5 wt% IFR/1.5 wt% K-TU passed UL-94 V-0 level, had a LOI of 35.4 %, and its peak heat release rate was reduced to 291 kW/m^2 from 1474 kW/m^2 of neat PP. The TGA results demonstrated that K-TU increased the thermal degradation onset temperature and enhanced the char formation of PP/IFR composites. Meanwhile, the mechanical performance of PP/IFR composite was improved by the presence of K-TU. It was proposed that the improved flame retardancy of PP composite was ascribed to both the shielding effect formed by exfoliated K-TU molecules and gas phase effect caused by inert gases mixture released from TU, which could prohibit the heat and oxygen transfer and dilute the concentration of combustible gases during burning.

Introduction

PP is highly combustible with severe dripping and leaves no char; its LOI is only 18 %, which restricts its applications in many fields. To overcome these problems, much work has been done [1–5].

Furthermore, it has been reported that natural clay including layered double hydroxides (LDHs), montmorillonite (MMT), halloysites (HNTs) [6–8], and kaolinite (K) can improve flame retardancy of PP [9].

Kaolinite has attracted more and more attention for it is abundant, low cost, and shielding effect in

polymer. Although the chemical composition of K is similar to HNTs, it differs by having a predominantly plate-like structure. Meanwhile, dissimilar to LDHs and MMT, K shows an asymmetric structure with the superposition of the tetrahedral (Al–O$_4$) and octahedral (Si–O$_8$) sheets in 1:1 layers [10, 11]. The stacked layers are linked by strong hydrogen bonds. Consequently, the asymmetry makes intercalation of K become more challenging than LDHs and MMT. Generally, pre-intercalation with small or dipolar molecules is first used, and sequentially the target guest is introduced by displacing intercalated precursor [10–14].

The synergistic flame retardant effect of kaolinite/*intumescent flame retardants (IFR)* in PP had been found in our previous study [15]. However, to the best of our knowledge, only limited literature about introducing the intercalated K to improve the fire performance of PP has been found so far. In this work, a novel flame retardant (K-TU) was prepared by intercalation of thiourea (TU) into K. The structure of K-TU was characterized and its contribution to flame retardancy of PP/IFR was discussed.

Experimental

Materials

The commercial PP, with a melt flow index of 3 g/(10 min), was kindly provided by Sinopec Maoming Company (Maoming, China). Ammonium polyphosphate (APP) was purchased from Jin Ying Tai Chemical Co., Ltd (Jinan, China). Melamine (MA) was obtained from Jin Tong Le Tai Chemical Product Co., Ltd (Beijing, China). Pentaerythritol phosphate (PEPA) was a product of Victory Chemistry Co., Ltd (Zhangjiagang, China). Formaldehyde (POM), dimethylsulphoxide (DMSO), methanol (MOH), and TU were purchased from Beijing Chemical Factory (Beijing, China). The raw kaolinite, with a size range of 1 ~46 μm (mean size of 12 μm) and the specific surface area of 17 m^2/g (the purity >95 %), was kindly supplied by Xing Yi Mineral Processing Plant (Shijiazhuang, China).

Preparation of thiourea-intercalated kaolinite

Scheme 1 illustrates the 3-step process for the preparation of TU-intercalated kaolinite.

Step one: 4 g K was dispersed in a mixture of 40 mL DMSO and 4.5 mL deionized water. The suspension was subjected to ultrasonic waves with a power of 200 w for 4 h. The reacted mixture was washed three times with ethanol and then filtered before being drying at 60 °C for 12 h. The product obtained was DMSO-intercalated kaolinite (marked as K-DMSO).

Step two: 2 g K-DMSO was mixed with 40 mL methanol and stirred at room temperature for 7 days. The product obtained was MOH-intercalated K (marked as K-MOH).

Step three: 2 g K-MOH was dispersed in 40 mL saturated thiourea solution of MOH and stirred at 50 °C for 2 days. The reacted mixture was washed three times with ethanol and then filtered before being drying at 60 °C for 12 h. The product obtained was TU-intercalated K (marked as K-TU).

Preparation of PP composites

PP and flame retardant were melt blended by a micro twin-screw extruder (Wuhan Rui Ming Plastics Machinery Co. Ltd). The processing temperature range from hopper to die was fixed at 170, 180, and 190 °C, respectively. The total amount of flame retardant additives was fixed at 25 wt%, consisting of IFR (MCAPP/PEPA = 2/1, 23.5 wt%) and K/K-TU (1.5 wt%).

Measurements

The X-ray diffraction (XRD) was performed with a D/max-2500 diffractometometer using Cu Kα radiation source at 40 kV and 20 mA ($\lambda = 0.154$ nm). The interlayer space of clay was calculated according to Bragg's Eq. (1).
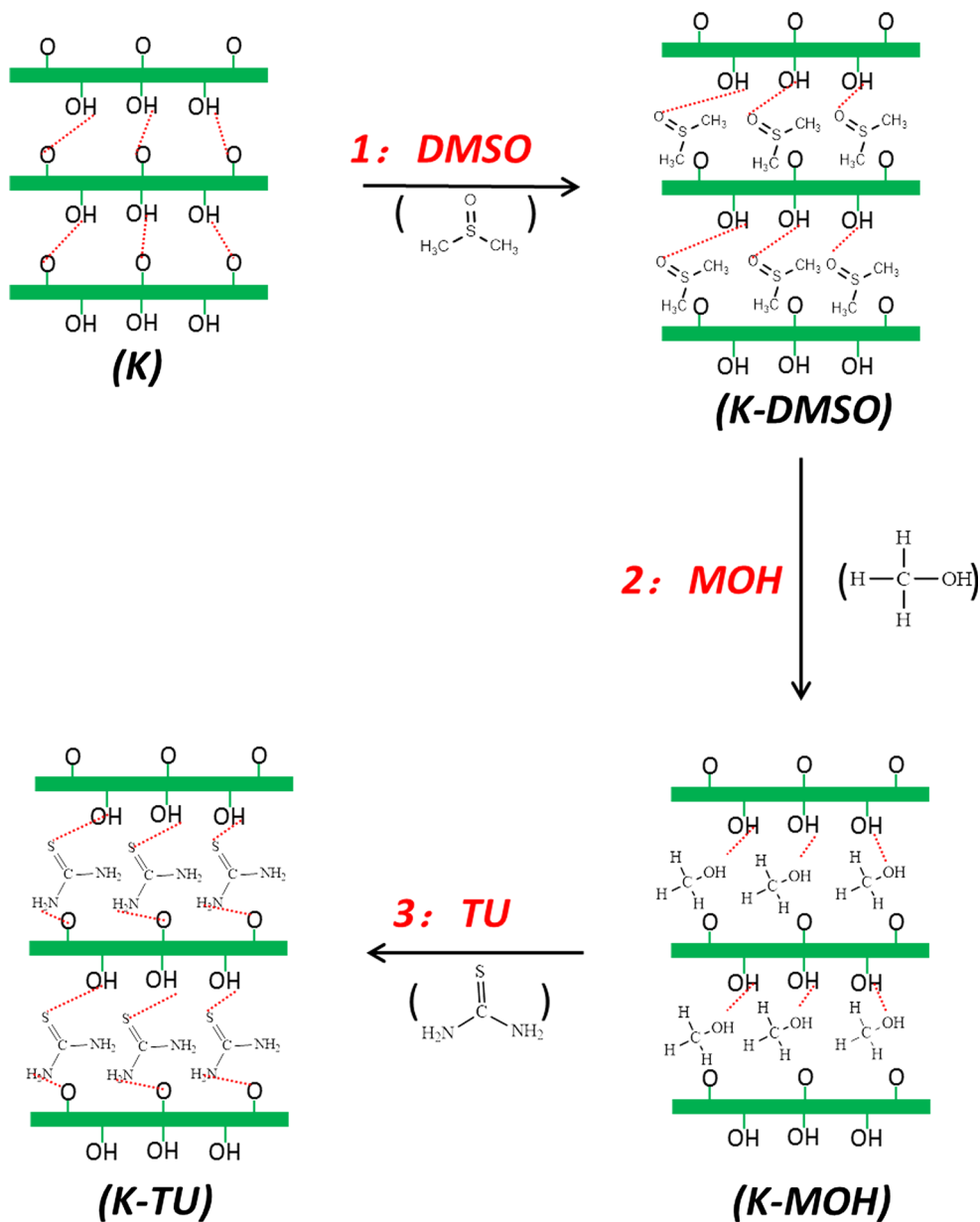
$$\lambda = 2d \sin \theta, \tag{1}$$

where d is the basal spacing and θ is the diffraction angle.

The percentage of intercalation is calculated according to Eq. (2):

$$Percentage\ of\ Intercalation = \frac{I_{i(001)}}{I_{i(001)} + I_{k(001)}} \times 100\ \%, \tag{2}$$

where $I_{k(001)}$ and $I_{i(001)}$ are the peak intensity of raw kaolinite and intercalated products, respectively.

Scheme 1 Preparation process for TU-intercalated K (K-TU).

Fourier transform infrared spectroscopy (FTIR) spectra were recorded in the 4000–500 cm^{-1} spectral region using a Nicolet IS5 under the resolution of 1 cm^{-1} in 32 scans.

Thermogravimetric analysis (TGA) was conducted using a synchronous thermal analyzer (STA449C, Netzsch) from 30 to 800 °C at a heating rate of 10 °C/min under nitrogen atmosphere. The mass for each sample was around 10 mg.

The micrographs of scanning electron microscopy (SEM) were obtained by a Hitachi S-4700 SEM under the voltage of 20 kV.

The limiting oxygen index (LOI) was tested by JF-3 oxygen index apparatus (Jiangning Nanjing Analytical Instrument Co. Ltd) according to the oxygen index test method of ISO 4589-2. The dimension of each sample was 50 × 6.5 × 3 mm^3.

The vertical burning behavior (UL-94) was measured by a CZF-3 apparatus (Jiangning Nanjing Analytical Instrument Co. Ltd) according to the ASTM D 3801 standard. The dimension of each sample was 130 × 13 × 3 mm^3.
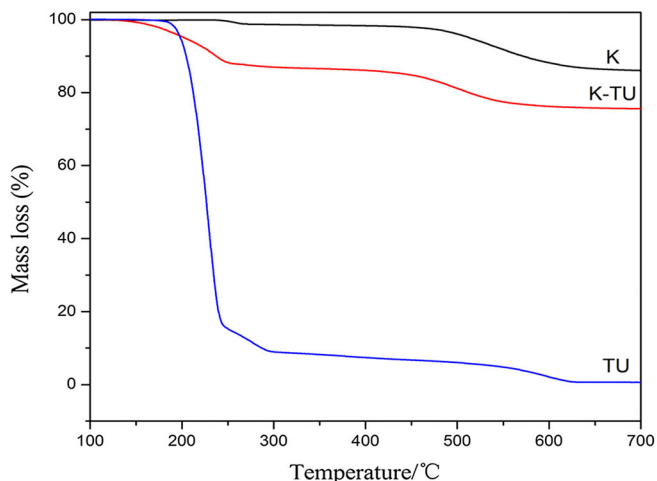
Cone calorimetry (FTT Co., Ltd) was performed according to the standard ISO 5660 method. The
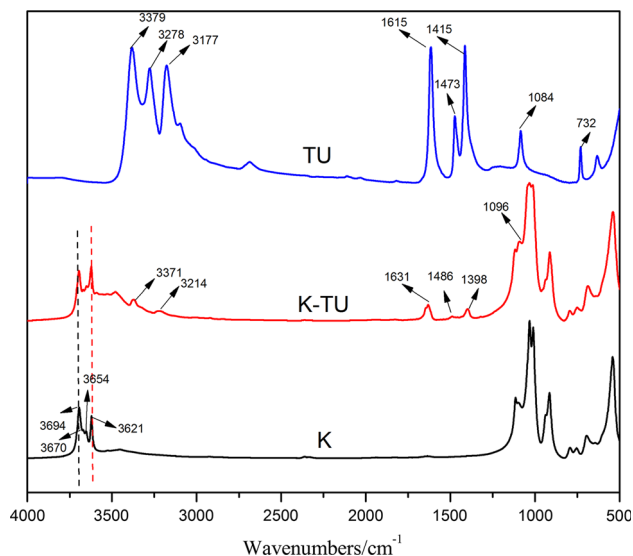
Figure 1 FTIR spectra of K, TU, and K-TU.

Results and discussion

Characterization of K-TU

Figure 1 shows the FTIR spectra of K, TU, and K-TU. It shows that K contains two types of –OH [11, 15]: the absorption bands at 3694, 3670, and 3654 cm^{-1} corresponded to interlayer –OH stretching, while the band at 3621 cm^{-1} was attributed to the internal –OH. In TU, the bands at 3379, 3278, and 3177 cm^{-1} were attributed to the –NH$_2$, whereas bands at 1615, 1473, 1415, 1084, and 732 cm^{-1} were attributed to the N$_2$–C=S group [16–18]; all these special bands of TU remained in K-TU but moved a little from their original positions. The results indicated that TU was intercalated into K and could form some chemical bonds. Based on the chemical composition of TU and K, there exists high possibility to form two kinds of hydrogen bonds (S···H–O and N–H···O).

Figure 2 presents the TGA curves of K, TU, and K-TU. The DTG curve of K showed a minor mass loss during 220–280 °C, attributing to the elimination of water of crystallization in the interlayers of K, and a major mass loss during 480–580 °C in TGA curve, corresponding to the peak at 543 °C, which was attributed to the main dehydroxylation process [11, 19]. The TGA curve of TU showed a major mass loss step during 200–300 °C, centering at 230 °C. K-TU exhibited two major mass losses: the former was the decomposition of TU, and the latter one during 450–600 °C, centering at 496 °C, was the

samples with a dimension of 100 × 100 × 3 mm^3 were tested at horizontal position with heat radiant flux density of 50 kW/m^2. Specimens were wrapped in aluminum foil, leaving the upper surface exposed to the radiator, and then placed on ceramic backing board at a distance of 25 mm from the cone heater base. The experiments were repeated three times.

The tensile testing was carried out using a tensile tester (Zwick/Roell, Germany) at ambient temperature with a stretching rate of 50 mm/min according to the ISO 527-2 standard.
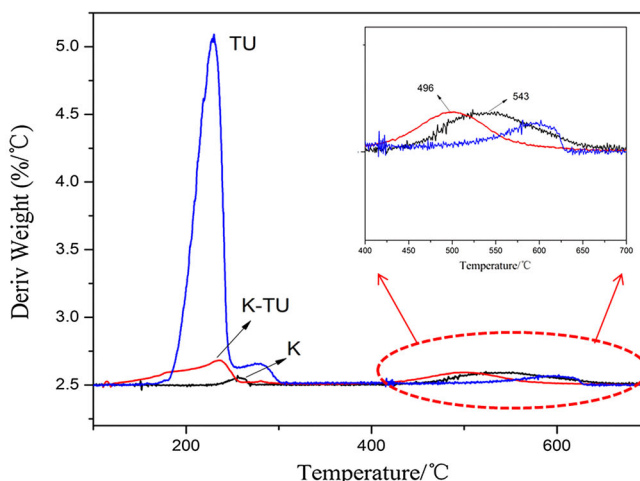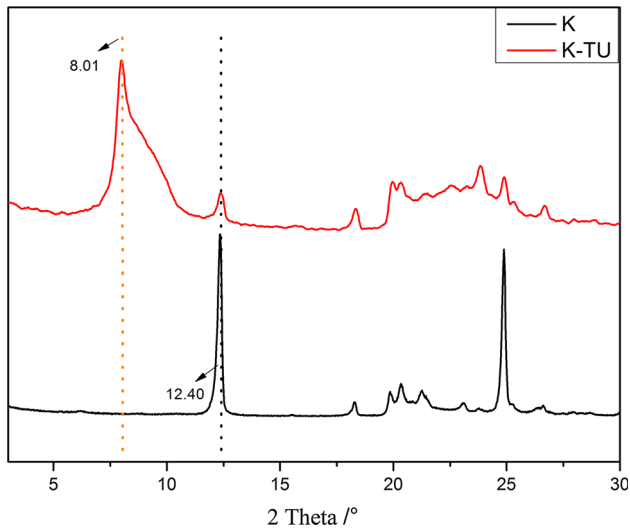

Figure 2 TGA and DTG curves of K, TU, and K-TU.

Figure 3 XRD patterns of K, TU, and K-TU.

dehydroxylation of K. Meanwhile, the dehydroxylation temperature of K-TU (496 °C) was lower than that of K (543 °C), which was associated with the obvious enlargement of the first mass loss step in K-TU.

Figure 3 shows the XRD patters of K, TU, and K-TU. The diffraction peak of d_{001} left shifted from 12.4° in K to 8.01° in K-TU, indicating that interplanar spacing increased from 0.72 to 1.11 nm. The percentage of intercalation of K-TU was 82.6 %, which indicated that TU had been intercalated into clay layers. On the other hand, the peak breadth of d_{001} was obviously widened in K-TU, which indicated that the size of crystal particle was sharply decreased based on the Scherrer rule. The most likely reason was that the H-bond in interlayers was disrupted and the large K particles were fragmented. Smaller sizes favor better distribution of K-TU in PP.
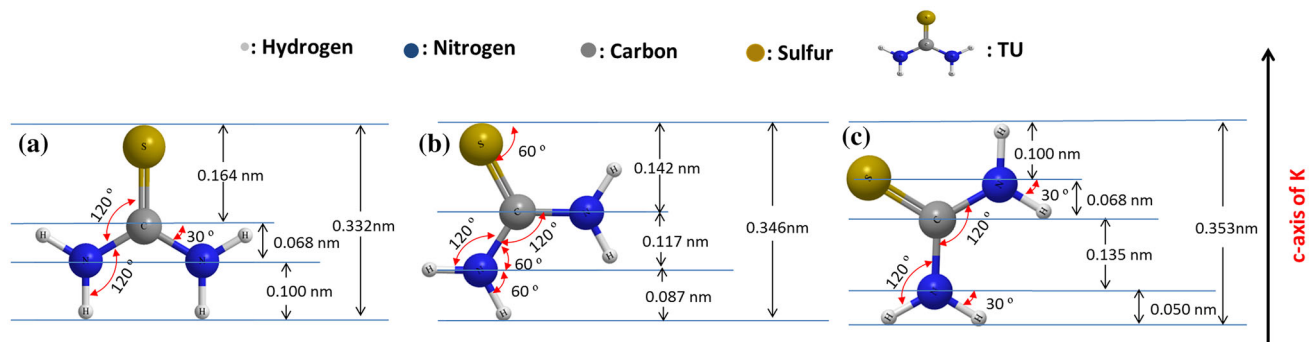
Possible chemical structure of K-TU

The d_{001} spacing of K increased from 0.72 to 1.11 nm in K-TU, indicating about 0.39 nm increment in the interlayer spacing. According to the literature [18], the equilibrium bond lengths of S=C, C–N, and N–H in TU were 0.164, 0.135, and 0.100 nm, respectively, as well as all the bond angles were 120°. As shown in Fig. 4a, when the TU molecules are parallel to the c-axis of K, the height occupied is minimum, of about 0.332 nm; as shown in Fig. 4b and c, when the C–N groups are perpendicular or parallel to the c-axis of K, the heights occupied by the TU molecules were 0.346 or 0.353 nm, respectively. Regardless of any kind of state, there will exist a gap around 0.04 nm. Therefore, a question arises as to how this gap may be filled. Perhaps, the most sensible assumption was that the –NH$_2$ and S=O groups have formed hydrogen bonds with the –OH groups in the interlayers of K. Meanwhile, FTIR results above suggest that there maybe exist two kinds of hydrogen bond. Therefore, the possible structure of K-TU proposed is shown in Fig. 5.

Dispersion of kaolinite

Dispersion of K and K-TU in PP/IFR composites was observed by SEM (Fig. 6). It can be seen that in PP/IFR composite, the average size of K particles was about 15 μm, but K-TU particle was generally less than 5 μm. It was shown that K-TU particles scattered were smaller in size compared to K particles.

The XRD patterns of PP composites are shown in Fig. 7. It was obviously noticed that the 001 lattice plane of K ($2\theta = 12.4°$) still existed in the PP/IFR/K, which demonstrated that the patterns of K had changed little in PP composite. However, the 001
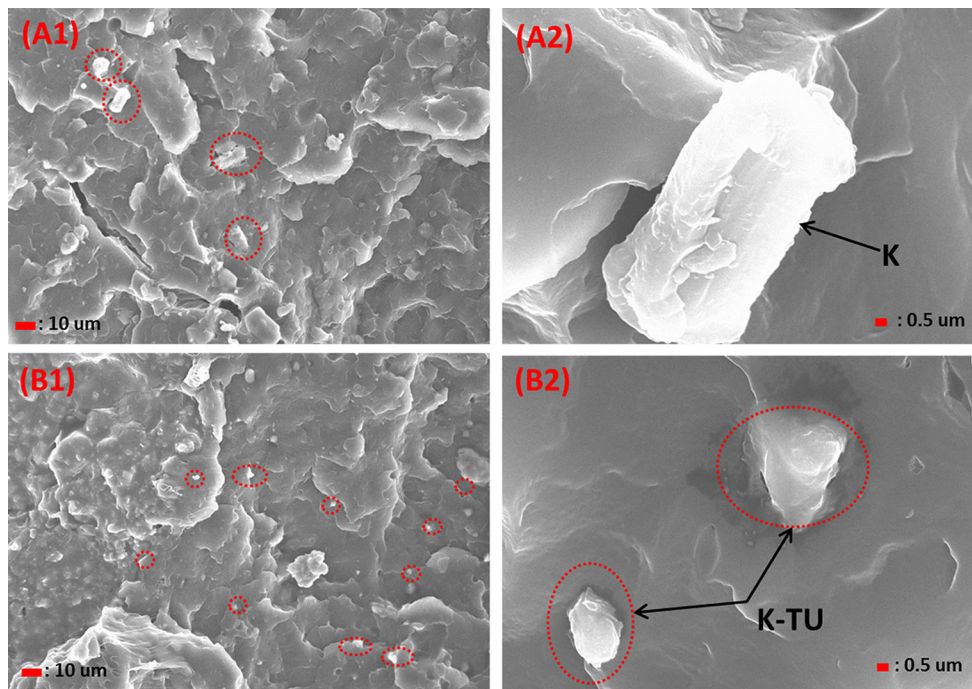

Figure 4 The possible arrangement mode of TU in K **a** C=S group is parallel to the c-axis of K, **b** C-N group is perpendicular to the c-axis of K, **c** C-N group is parallel to the c-axis of K.
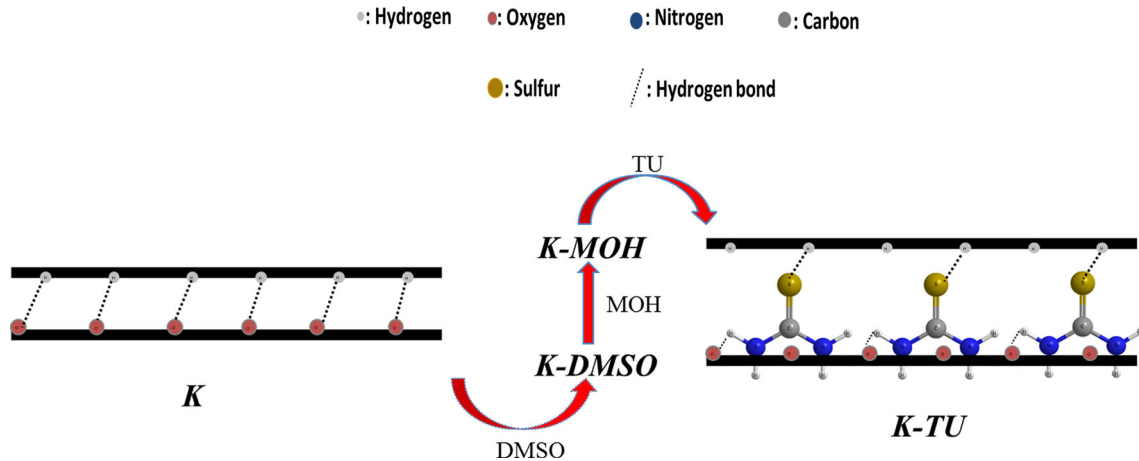
Figure 5 The possible chemical structure of K-TU.

Figure 6 SEM images of PP composites: **a1**, **a2** PP/IFR/K; **b1**, **b2** PP/IFR/K-TU.

lattice plane of K-TU ($2\theta = 8.01°$) almost disappeared in the PP/IFR/K-TU, which indicated that K-TU was almost exfoliated in the composite.

Cone

Cone results are shown in Fig. 8 and some key data are summarized in Table 1.

As shown in Fig. 8a, neat PP burned very fast after ignition and had a very strong peak heat release rate (pHRR) of 1474 kW/m². After 25 wt% IFR was 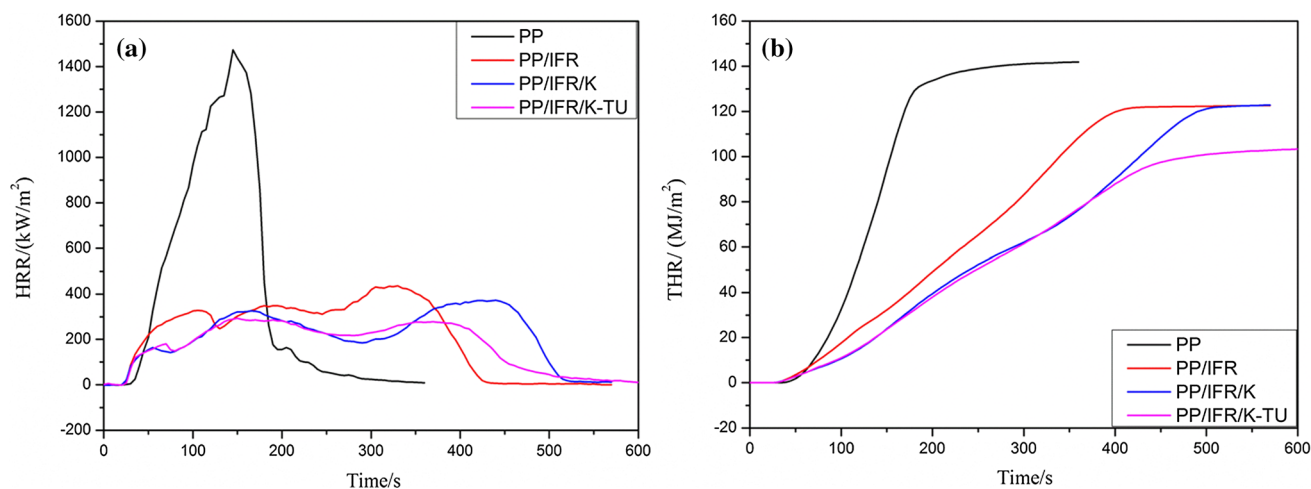introduced into PP, the pHRR value decreased sharply to 438 kW/m² accompanied with a remarkably prolonged combustion time, from about 250 s for neat PP to 420 s for PP/IFR. Moreover, the incorporation of 1.5 wt% K or K-TU into PP/IFR resulted in a further decrease of pHRR to 372 and 291 kW/m², respectively, and the whole combustion time exceeded 500 s. In other words, K-TU showed more efficient synergism than K. It was proposed that TU can release inert gases containing N, H, and S elements during combustion [17, 20, 21], which diluted the
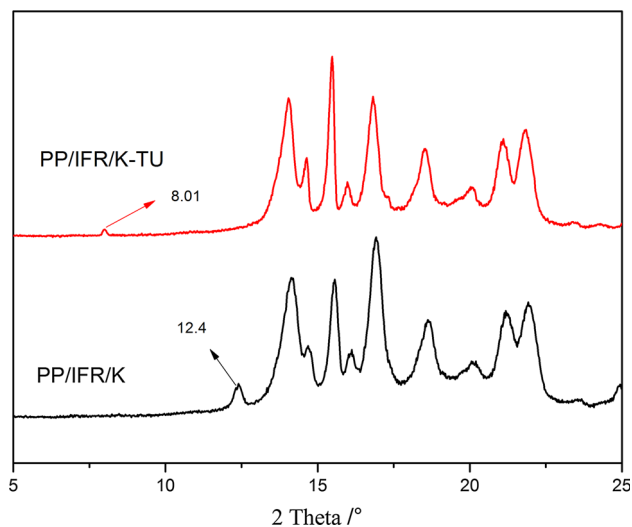
Figure 7 XRD patterns of PP/IFR/K and PP/IFR/K-TU.

concentration of combustible gases; on the other hand, smaller size and more uniform dispersion of K-TU than K was helpful to form more compact char which acted as a barrier to heat, oxygen, and other volatile gases during combustion [9, 21].

The total heat released (THR) curves of neat PP and its composites are shown in Fig. 8b. Generally, the slope of THR curve can be assumed as a representative of fire spread [22]. The THR value and its slope as a function of time were obviously decreased by the incorporation of 25 wt% IFR. Moreover, the slope was further decreased by the addition of K and K-TU. Especially, the THR value had reduced to 103 MJ/m^2 for the sample containing K-TU. It was proposed that K-TU can effectively reduce the heat release.

LOI and UL-94

The LOI values and UL-94 ratings of PP and its composites are presented in Table 2. Neat PP had a LOI value of only 18.0 %, and had no UL-94 rating. The LOI value increased to 31.1 % after the addition of 25 wt% IFR, however, and the UL-94 rating just reached V-2. It has been reported that the presence of clay can partly enhance the fire performance of polymer composite containing IFR [23–25]. After 1.5 wt% replacement of IFR with K, LOI increased slightly to 32.5 %. Furthermore, replacement of 1.5 wt% K-TU increased the LOI value to 35.4 %. Meanwhile, PP/IFR composites containing either K or K-TU achieved a V-0 rating.

Thermostability

The TGA curves of PP and its composites are shown in Fig. 9. The values of temperature corresponding to 10 % weight loss ($T_{10\%}$) and maximum weight loss rate (T_{max}), as well as the amount of residual char are provided in Table 3.

One-step decomposition during 400–500 °C with no residue left at high temperature (above 500 °C) was observed for PP. Two separate decomposition stages occurred in PP/IFR sample: the first one at 250–350 °C was caused by the earlier decomposition of IFR, which caused the $T_{10\%}$ occur at 404 °C compared to 431 °C in the case of neat PP. During this stage, H_2O and NH_3 were released by decomposition of IFR. However, the other step was prolonged to higher temperature (above 450 °C) compared to neat PP, which was assigned to the main decomposition of

Figure 8 Cone results of PP and its composites a HRR, b THR.

Table 1 Key cone calorimeter data of PP composite

	PP	PP/25 wt% IFR	PP/23.5 wt% IFR/1.5 wt% K	PP/23.5 wt% IFR/1.5 wt% K-TU
pHRR (kW/m^2)	1474	438	372	291
pSPR/(m^2/s)	0.110	0.082	0.079	0.058
THR/(MJ/m^2)	142	123	123	103
TSP/(m^2/m^2)	1655	2673	2612	1959
TTI/(s)	27	18	17	21
Residues/(%)	0	13.1	14.8	16.9

SPR smoke production rate, *THR* total heat released, *TSP* total smoke production, *TTI* time to ignition

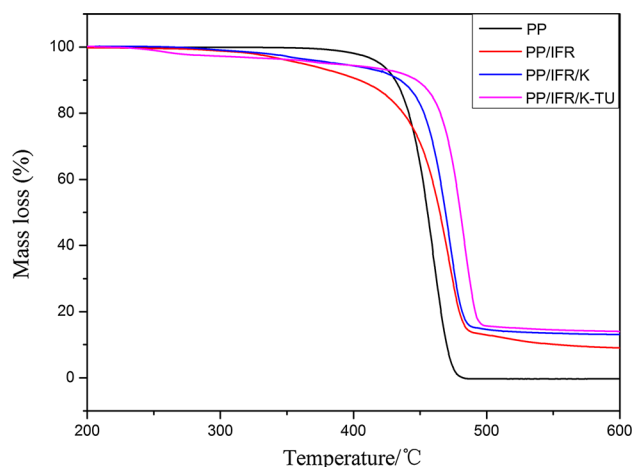**Table 2** Formulation, LOI, and UL-94 tests of PP composites

Samples	PP (wt%)	IFR (wt%)	K (wt%)	K-TU (wt%)	LOI (%)	UL-94
PP	100	–	–	–	18.1 ± 0.1	NR
PP/IFR	75	25	–	–	31.1 ± 0.2	V-2
PP/IFR/K	75	23.5	1.5	–	32.5 ± 0.2	V-0
PP/IFR/K-TU	75	23.5	–	1.5	35.4 ± 0.2	V-0

polymer matrix [26] and formed a final residue of about 9.1 wt% at 600 °C.

After 1.5 wt% replacement of IFR with K, the $T_{10\%}$ (431 °C) and final residue (13.2 %) of PP/IFR/K composite exhibited obvious improvement compared to that of PP/IFR composite. The results indicated that K restrained the decomposition of IFR in the first stage but showed minimal influence on controlling decomposition of PP matrix. Regardless, K significantly promoted the char content.

It was noted that $T_{10\%}$ and T_{max} of PP/IFR/K-TU increased to 448 and 483 °C, respectively. Meanwhile, the amount of residual char at 600 °C increased to 14.1 %. It was demonstrated that K-TU affected the decomposition of both IFR and PP, which consequently improved the thermal stability of PP composite. The promotion of K-TU on char formation was better than that of K.

Mechanical properties of PP composites

The tensile strength of neat PP and PP composites is displayed in Fig. 10. The tensile strength of neat PP was 35.3 MPa, and it decreased to 23.9 MPa by the introduction 25 wt% IFR. However, the tensile strength showed a slight increase after the introduction of K or K-TU. Both the larger surface area of K-TU and polar groups in TU promoted the interaction between filler and polymer, so K-TU acted as stress arrestor in the composite [27].

Figure 9 TGA curves of PP and its composites under N$_2$.

Table 3 Key data of TGA curves of PP composites

Samples	$T_{10\%}$/°C	T_{max}/°C	Residues (wt%)/$W_{600\,°C}$
PP	431	460	0
PP/IFR	404	472	9.1
PP/IFR/1.5 K	435	472	13.2
PP/IFR/1.5 K-TU	448	483	14.1
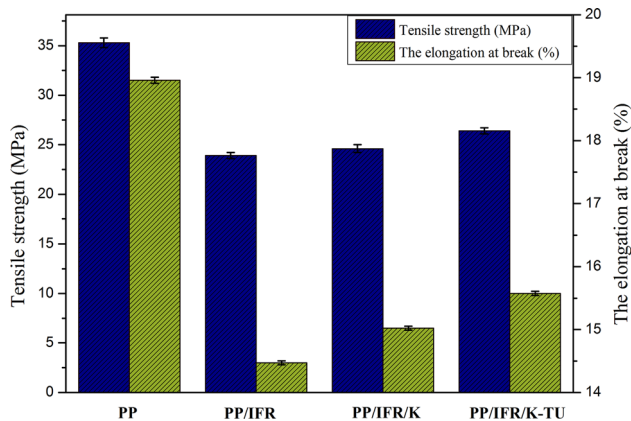
Figure 10 Tensile strength and the elongation at break of neat PP and its composites.

The elongation at break of PP composites showed similar trend to tensile strength. It was reduced from 18.9 % of neat PP to 14.5 % of PP/IFR composite, but was slightly increased to 15.1 and 15.5 % in the presence of K and K-TU, respectively.

Conclusion

A novel modified kaolinite, TU-intercalated kaolinite (K-TU) was successfully prepared by a three-step method. The contribution of K-TU on the flame retardancy of PP/IFR was documented by LOI, UL-94, and Cone. The flame retardant mechanism of K-TU in both gas phase and solid phase was proposed. K-TU promoted the formation of compact and continued char layers, which can restrain heat release and reduce the fire spread. Meanwhile, the tensile strength of PP/IFR was also slightly improved by the addition of K-TU.

Acknowledgements

References

[1] Zhang S, Horrocks AR (2003) A review of flame retardant polypropylene fibres. Prog Polym Sci 28(11):1517–1538. doi:10.1016/j.progpolymsci.2003.09.001

[2] Liu XS, Gu XY, Zhang S, Jiang Y, Sun J, Dong MZ (2013) Effects of dihydrogen phosphate intercalated layered double hydroxides on the crystal behaviors and flammability of polypropylene. J Appl Polym Sci 130(5):3645–3651. doi:10.1002/app.39614

[3] Dong MZ, Gu XY, Zhang S (2014) Effects of compound oxides on the fire performance of polypropylene composite. Ind Eng Chem Res 53(19):8062–8068. doi:10.1021/ie500178u

[4] Chen XL, Jiao CM (2009) Synergistic effects of hydroxy silicone oil on intumescent flame retardant polypropylene system. Fire Saf J 44(8):1010–1014. doi:10.1016/j.firesaf.06.008

[5] Pappalardo S, Russo P, Acierno D, Rabe S, Schartel B (2016) The synergistic effect of organically modified sepiolite in intumescent flame retardant polypropylene. Eur Polym J 76:196–207. doi:10.1016/j.eurpolymj.2016.01.041

[6] Wang LJ, He XJ, Lu HD, Feng JX, Xie XL, Su SP, Wikie CA (2011) Flame retardancy of polypropylene (nano)composites containing LDH and zinc borate. Polym Adv Technol 22(7):1131–1138. doi:10.1002/pat.1927

[7] Liu Y, Wang JS, Deng CL, Wang DY, Song YP, Wang YZ (2010) The synergistic flame-retardant effect of O-MMT on the intumescent flame-retardant PP/CA/APP systems. Polym Adv Technol 21(11):789–796. doi:10.1002/pat.1502

[8] Lecouvet B, Sclavons M, Bailly C, Bourbigot S (2013) A comprehensive study of the synergistic flame retardant mechanisms of halloysite in intumescent polypropylene. Polym Degrad Stabil 98(11):2268–2281. doi:10.1016/j.polymdegradstab.2013.08.024

[9] Tang WF, Gu XY, Jiang Y, Zhao JR, Ma WJ, Jiang P, Zhang S (2015) Flammability and thermal behaviors of polypropylene composite containing modified kaolinite. J Appl Polym Sci. doi:10.1002/app.41761

[10] Zhang L, Wang CJ, Yan ZF, Wu XL, Wang YQ, Meng DW, Xie HX (2013) Kaolinite nanomaterial: intercalation of 1-butyl-3-methylimidazolium bromine in a methanol–kaolinite pre-intercalate. Appl Clay Sci 86:106–110. doi:10.1016/j.clay.2013.07.003

[11] Cheng HF, Liu QF, Yang J, Ma SJ, Frost RL (2012) The thermal behavior of kaolinite intercalation complexes-A review. Thermochim Acta 545:1–13. doi:10.1016/j.tca.2012.04.005

[12] Yuan P, Tan DY, Annabi-Bergaya F, Yan WC, Liu D, Liu ZW (2013) From platy kaolinite to alumino silicate nanoroll via one-step delamination of kaolinite: effect of the temperature of intercalation. Appl Clay Sci 83–84:68–76. doi:10.1016/j.clay.2013.08.027

[13] Li YF, Zhang B, Pan XB (2008) Preparation and characterization of PMMA—kaolinite intercalation composites.

Comp Sci Tech 68(9):1954–1961. doi:10.1016/j.compsci tech.2007.04.003

[14] Sun DW, Li YF, Zhang B, Pan XB (2010) Preparation and characterization of novel nanocomposites based on poly-acrylonitrile/kaolinite. Comp Sci Tech 70(6):981–988. doi:10.1016/j.compscitech.2010.02.016

[15] Zhang S, Jiang P, Liu XS, Gu XY, Zhao Q, Hu ZW, Tang WF (2014) Effects of kaolin on the thermal stability and flame retardancy of polypropylene composite. Polym Adv Technol 25:912–919. doi:10.1002/pat.3325

[16] Singh G, Saroa A, Rani S, Promila A, Girdhar S, Sahoo S, Choquesillo-Lazarte D (2016) Substituted phenyl urea and thiourea silatranes: synthesis, characterization and anion recognition properties by photophysical and theoretical studies. Polyhedron 112:51–60. doi:10.1016/j.poly.2016.03.036

[17] Fujimori T, Nakamura M, Takaoka M, Shiota K, Kitajima Y (2016) Synergetic inhibition of thermochemical formation of chlorinated aromatics by sulfur and nitrogen derived from thiourea: multielement characterizations. J Hazard Mater 311:43–50. doi:10.1016/j.jhazmat.02.054

[18] Yamaguchi A, Penland RB, Mizushima S, Lane TJ, Curran C, Quagliano JV (1958) Infrared absorption spectra of inorganic coordination complexes. XIV. Infrared studies of some metal thiourea complexes. J Am Chem Soc 80:527–529. doi:10.1021/ja01536a005

[19] Zhang XR, Xu Z (2007) The effect of microwave on preparation of kaolinite/dimethyl sulfoxide composite during intercalation process. Mat Let 61(7):1478–1482. doi:10.1016/j.matlet.2006.07.057

[20] Wang ZD, Yoshida M, George B (2013) Theoretical study on the thermal decomposition of thiourea. Comput Theor Chem 1017:91–98. doi:10.1016/j.comptc.2013.05.007

[21] Tang WF, Zhang S, Sun J, Gu XY (2016) Flame retardancy and thermal stability of polypropylene composite containing ammonium sulfamate intercalated kaolinite. Ind Eng Chem Res 55(28):7669–7678. doi:10.1021/acs.iecr.6b01722

[22] Almeras X, Bras ML, Hornsby P, Bourbigot S, Marosi G, Keszei S, Poutch P (2003) Effect of fillers on the fire retardancy of intumescent polypropylene compounds. Polym Degrad Stab 82(2):325–331. doi:10.1016/S0141-3910(03)00187-3

[23] Tang Y, Hu Y, Wang S, Gui Z, Chen Z, Fan W (2003) Intumescent flame retardant montmorillonite synergism in polypropylene-layered silicate nanocomposites. Polym Int 52(8):1396–1400. doi:10.1002/pi.1270

[24] Ren Q, Zhang Y, Li J, Li JC (2011) Synergistic effect of vermiculite on the intumescent flame retardance of polypropylene. J Appl Polym Sci 120(2):1225–1233. doi:10.1002/app.33113

[25] Du B, Ma H, Fang Z (2011) How nano-fillers affect thermal stability and flame retardancy of intumescent flame retarded polypropylene. Polym Adv Technol 22(7):1139–1146. doi:10.1002/pat.1914

[26] Feng C, Zhang Y, Liu SW, Chi ZG, Xu JR (2012) Synergistic effect of La_2O_3 on the flame retardant properties and the degradation mechanism of a novel PP/IFR system. Polym Degrad Stabil 97(5):707–714. doi:10.1016/j.polymdegradstab.2012.02.014

[27] Zhu SP, Chen JY, Zuo Y, Li HL, Cao Y (2011) Montmo-rillonite/polypropylene nanocomposites: mechanical properties, crystallization and rheological behaviors. Appl Clay Sci 52(1–2):171–178. doi:10.1016/j.clay.2011.02.021